Assessment of the long-lead probabilistic prediction for the Asian summer monsoon precipitation (1983–2011) based on the APCC multimodel system and a statistical model

Soo-Jin Sohn,[1,2] Young-Mi Min,[1] June-Yi Lee,[3] Chi-Yung Tam,[4] In-Sik Kang,[5] Bin Wang,[3] Joong-Bae Ahn,[2] and Toshio Yamagata[6]

Received 25 May 2011; revised 13 December 2011; accepted 14 December 2011; published 17 February 2012.

[1] The performance of the probabilistic multimodel prediction (PMMP) system of the APEC Climate Center (APCC) in predicting the Asian summer monsoon (ASM) precipitation at a four-month lead (with February initial condition) was compared with that of a statistical model using hindcast data for 1983–2005 and real-time forecasts for 2006–2011. Particular attention was paid to probabilistic precipitation forecasts for the boreal summer after the mature phase of El Niño and Southern Oscillation (ENSO). Taking into account the fact that coupled models' skill for boreal spring and summer precipitation mainly comes from their ability to capture ENSO teleconnection, we developed the statistical model using linear regression with the preceding winter ENSO condition as the predictor. Our results reveal several advantages and disadvantages in both forecast systems. First, the PMMP appears to have higher skills for both above- and below-normal categories in the six-year real-time forecast period, whereas the cross-validated statistical model has higher skills during the 23-year hindcast period. This implies that the cross-validated statistical skill may be overestimated. Second, the PMMP is the better tool for capturing atypical ENSO (or non-canonical ENSO related) teleconnection, which has affected the ASM precipitation during the early 1990s and in the recent decade. Third, the statistical model is more sensitive to the ENSO phase and has an advantage in predicting the ASM precipitation after the mature phase of La Niña.

Citation: Sohn, S.-J., Y.-M. Min, J.-Y. Lee, C.-Y. Tam, I.-S. Kang, B. Wang, J.-B. Ahn, and T. Yamagata (2012), Assessment of the long-lead probabilistic prediction for the Asian summer monsoon precipitation (1983–2011) based on the APCC multimodel system and a statistical model, *J. Geophys. Res.*, *117*, D04102, doi:10.1029/2011JD016308.

1. Introduction

[2] The multimodel ensemble (MME) approach was developed for quantifying forecast uncertainties that stem from model formulations [*Krishnamurti et al.*, 1999, 2000; *Doblas-Reyes et al.*, 2000; *Shukla et al.*, 2000; *Palmer et al.*, 2000], and has been recognized as an effective tool to improve dynamical weather and climate forecasts. Indeed, this approach is used by several major operational centers for seasonal climate prediction [*Palmer et al.*, 2004; *Climate Test Bed*, 2006; *Lee et al.*, 2009]. In particular, since 2006, the Asia-Pacific Economic Cooperation (APEC) Climate Center (APCC) has produced long-range seasonal forecasts with up to a six-month lead time using an MME of coupled ocean–atmosphere–land models for use by National Hydrological and Hydrometeorological Services within the APEC [*Lee et al.*, 2009].

[3] Using historical retrospective forecast data (usually referred to as hindcast, as shown by *Graham et al.* [2005], *Palmer et al.* [2004], and *Wang et al.* [2009]), most previous studies focused on deterministic long-lead coupled predictions [*Wang et al.*, 2008; *Liang et al.*, 2009; *Chowdary et al.*, 2010; *Lee et al.*, 2010; *S. S. Lee et al.*, 2011]. However, climate forecasts are known to be associated with uncertainties, which can be quantified in terms of probabilities. Thus, probabilistic forecasts not only provide more useful information but are also of greater value to end users for decision-making [*Murphy*, 1977; *Krzysztofowicz*, 1983; *Palmer et al.*, 2004; *Richardson*, 2006; *Alessandri et al.*, 2011]. Generalizing the concept to MME predictions, APCC has recently developed a probabilistic seasonal prediction system based on MME outputs [*Min et al.*, 2009; Y. M. Min et al., Improvement of the APCC probabilistic

[1]APEC Climate Center, Busan, South Korea.
[2]Department of Atmospheric Sciences, Pusan National University, Busan, South Korea.
[3]International Pacific Research Center and Department of Meteorology, University of Hawai'i at Mānoa, Honolulu, Hawaii, USA.
[4]Guy Carpenter Asia-Pacific Climate Impact Centre, City University of Hong Kong, Hong Kong.
[5]Climate Environment System Research Center, Seoul National University, Seoul, South Korea.
[6]Department of Earth and Planetary Science, University of Tokyo, Tokyo, Japan.

0148-0227/12/2011JD016308

Table 1. Acronyms and Description of Models Used in This Study

Institute	Model	AGCM	Resolution	OGCM	Resolution	Ensemble Member	Reference
APCC	CCSM3[a]	CAM3[b]	T85 L26	POP1.3	gxlv3 L40	5	*Jeong et al.* [2008]
NCEP[c]	CFS[d]	GFS[e]	T62 L64	MOM3	1/3° lat × 5/8° lon L27	15	*Saha et al.* [2006]
FRCGC[f]	SINTEX-F[g]	ECHAM4[h]	T106 L19	OPA 8.2	2°cos(lat) × 2°lon L31	9	*Luo et al.* [2005]
SNU[i]	SNU	SNU	T42 L21	MOM2.2	1/3° lat × 1° lon L32	6	*Ham and Kang* [2010]

[a]Community Climate System, version 3.0.
[b]Community Atmospheric Model, version 3.0.
[c]National Centers of Environmental Prediction.
[d]Climate Forecast System.
[e]Global Forecast System.
[f]Frontier Research Center for Global Change.
[g]Scale INTeraction Experiment-FRCGC.
[h]The fourth-generation atmospheric general circulation model of European Centre for Medium-Range Weather Forecasts–Deutsches Klimarechenzentrum: Hamburg.
[i]Seoul National University.

multi-model seasonal prediction by model calibration and combination, submitted to *Climate Dynamics*, 2011].

[4] Overall, state-of-the-art coupled models have shown significantly high skill in ENSO predictions with lead times of six months and beyond [*Jin et al.*, 2008; *Wang et al.*, 2009]. On the other hand, it is known that such climate models generally have difficulties in predicting the summer mean precipitation over the Asian summer monsoon (ASM) region, even with a one-month lead time [*Wang et al.*, 2007, 2008, 2009; *Kug et al.*, 2008; *Lee et al.*, 2010; *S. S. Lee et al.*, 2011]. However, recent studies suggest that model prediction skill for the summer precipitation tends to increase after the mature phase of El Niño and Southern Oscillation (ENSO), particularly over East Asia and the western North Pacific (WNP) monsoon region [*Wang et al.*, 2009; *Liang et al.*, 2009; *Chowdary et al.*, 2010; *J.-Y. Lee et al.*, 2011; *S. S. Lee et al.*, 2011; *Lee and Wang*, 2012]. Thus, the lagged impact of ENSO on the ASM precipitation can be exploited for developing a statistical prediction model.

[5] Numerical models that represent the dynamics of the atmosphere, ocean, and land should be able to give better seasonal forecasts than purely statistical approaches, because of their ability to handle a wide range of linear and nonlinear interactions and their potential resilience to the changing climate [*van Oldenborgh et al.*, 2005]. Nonetheless, statistical methods are still widely used in seasonal predictions and, in some cases, tend to have prediction skills comparable to those of dynamical models [*Anderson et al.*, 1999; *Barnston et al.*, 1999; *van Oldenborgh et al.*, 2005]. Furthermore, statistical forecasts also have an advantage in that knowledge obtained from data analysis can be easily applied. However, application of the statistical approach to long-lead prediction requires careful use of conventional statistical modeling techniques, in particular, due to the relatively short history of the observed database and the existence of long-term changes in the climate system. It is therefore worthwhile to investigate the extent to which such a physically based statistical model can outperform dynamical models in predicting the ASM precipitation.

[6] With this motivation, the present study aims at evaluating the long-lead probabilistic multimodel prediction (PMMP) system of APCC assembled from four coupled models initiated in February for the real-time forecast period of 2006–2011 as well as the hindcast period of 1983–2005, focusing on the ASM precipitation prediction after the mature phase of ENSO. The rest of this paper is organized as follows. Section 2 describes the coupled models and their hindcasts being considered, and the observational data and methodology used in the present study. Verification of the PMMP for the ASM precipitation in terms of reliability diagrams and relative operating characteristic score (ROCS) for the hindcast period is presented in section 3. Verification of a regression-based statistical model for the same period is shown in section 4. Section 5 compares the real-time forecast skill (2006–2011) of the dynamical and statistical models for the ASM precipitation. Finally, the results are summarized and their significance is discussed in section 6.

2. Data and Methodology

2.1. The APCC PMMP System

[7] APCC launched its six-month-lead seasonal climate prediction using four ocean–atmosphere–land coupled models (Table 1), which is issued four times a year. For this study, predictions for the seasons of March–April–May (MAM) and June–July–August (JJA) are evaluated, with the coupled models initiated in February. All coupled model hindcast experiments cover the 23-year period of 1983–2005, and their real-time forecasts for the six-year period of 2006–2011 are also considered. The PMMP is constructed based on an uncalibrated multimodel approach, with model weights inversely proportional to the errors in the forecast probability associated with the model sampling errors [*Min et al.*, 2009], and a non-parametric empirical ranking method for estimating tercile-based categorical probabilities.

2.2. Statistical Model

[8] Motivated by the fact that the ASM precipitation tends to be more predictable after the mature phase of ENSO, we developed a regression-based statistical model with the ENSO condition in the preceding boreal winter as the predictor. The conditional probability P(B|A) is defined as the transfer function of the predictand and the predictor. This conditional probability is the probability of some event B, given the occurrence of some other event A; for our case, A is the preceding winter ENSO condition (defined as the value of the Niño 3.4 index; see section 2.3) and B represents the impact of an ENSO event on the ASM rainfall. In other words, the probabilistic composites are formulated

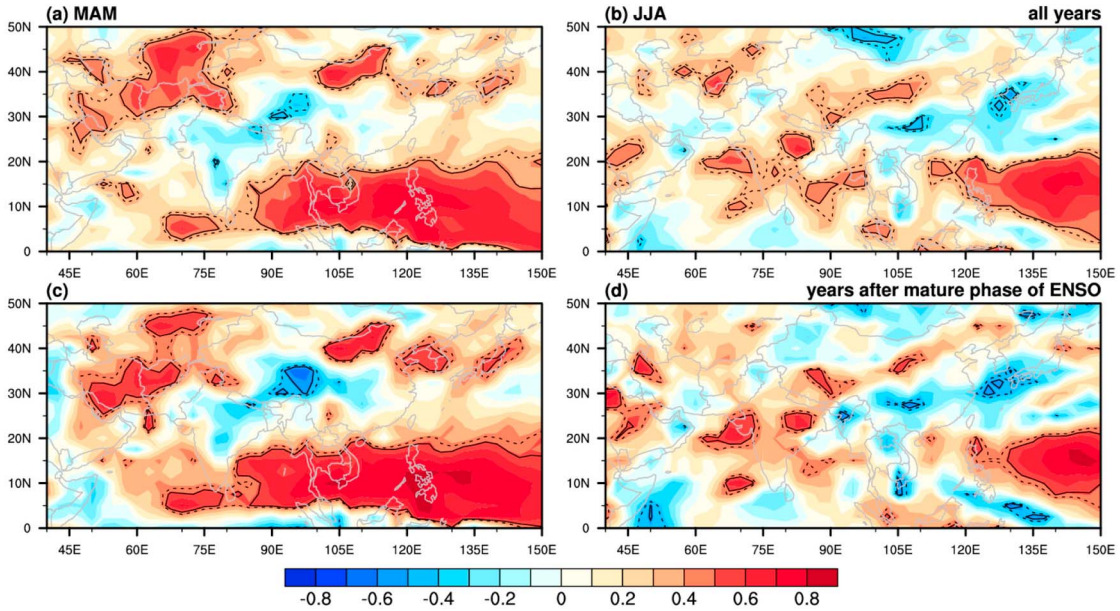

Figure 1. TCC between observations and the MME prediction for (a, c) MAM and (b, d) JJA precipitation during all years (Figures 1a and 1b) and years after mature phase of ENSO (Figures 1c and 1d). Dashed and solid lines denote the threshold values for the 90% and 95% confidence levels, respectively.

based on the probabilities of the ASM rainfall for ENSO in a given state such as El Niño (totally 7 years), La Niña (8 years), and the neutral state (8 years) during the training period. In a cross-validated mode, the precipitation field for the forecast year is not reflected in the composite.

[9] The statistical forecast model is constructed as follows. First, the probability of the Niño 3.4 index is estimated as a portion of the climatological probability distribution function of the indices during the training or cross-validated hindcast period. The probability P_B of the predictand B is computed as follows:

$$P_B(E_j) = \sum_{i=1}^{3} P_{B|A}(E_j) P_A(E_i)$$

where P_A is the probability of the predictor A, and E_j and E_i are the j and i events respectively [in this case the above normal (AN), near normal (NN), or below normal (BN) categories]. For our statistical model, the probabilistic forecast field for the ASM precipitation is then calculated by combining the probability of the status of ENSO (P_A) with the associated composite maps ($P_{B|A}$). Finally, in order to compare the statistical with the dynamical forecast, we produced a cross-validated statistical forecast for the 23 years from 1983 to 2005, as well as an independent forecast covering 2006–2011 (with 1983–2005 being the training period).

2.3. Observational Data Sets

[10] The observed precipitation data used in this study are the Climate Anomaly Monitoring System (CAMS) and Outgoing Longwave Radiation (OLR) Precipitation Index (OPI) product (CAMS OPI [*Janowiak and Xie*, 1999]). CAMS OPI is a precipitation analysis created by merging observations from rain gauges with satellite estimates to obtain the monthly mean global precipitation in quasi real time. CAMS OPI was found to be reliable for monitoring large-scale precipitation variation over the East Asian sector [*Sohn et al.*, 2012]. This rainfall data set is used to assess model forecasting skills and form the probabilistic composite maps for ASM precipitation based on the Niño 3.4 index. All data used in this study are interpolated onto a 2.5° × 2.5° grid.

[11] To define the ENSO condition, the Niño 3.4 index is used, which is obtained from the optimum interpolation (OI) of sea surface temperature (SST) data [*Reynolds et al.*, 2002]. Periods during which the standardized value of the DJF Niño 3.4 index is greater than 0.5 are identified as El Niño events; they are the winters of 1982/83, 1986/87, 1987/88, 1991/92, 1994/95, 1997/98, 2002/03, and 2009/10. The boreal winters of 1983/84, 1984/85, 1985/86, 1988/89, 1995/96, 1998/99, 1999/2000, 2000/2001, 2005/06, 2007/08, 2008/09, and 2010/11, when the Niño 3.4 index is less than −0.5, are identified as La Niña events.

2.4. Probabilistic Forecast Assessments

[12] To evaluate the forecast skills, we use reliability (attributes) diagrams [*Murphy*, 1973; *Murphy and Winkler*, 1977; *Wilks*, 1995; *Jolliffe and Stephenson*, 2003; *Atger*, 2003, 2004], the relative operating characteristic (ROC [*Swets*, 1973; *Mason*, 1982; *Wilks*, 1995; *Mason and Graham*, 1999; *Richardson*, 2000; *Zhu et al.*, 2002]) curves, and the area under the ROC curve (ROCS hereafter [*Green and Swets*, 1966]), following the recommendations of the World Meteorological Organization (WMO) Standardized Verification System for Long-Range Forecasts (SVS–LRF [*World Meteorological Organization*, 2002]; further details are given by *Min et al.* [2009]). The reliability diagram presents the relative frequency of an observed event against the forecast probability of the event for the bins into

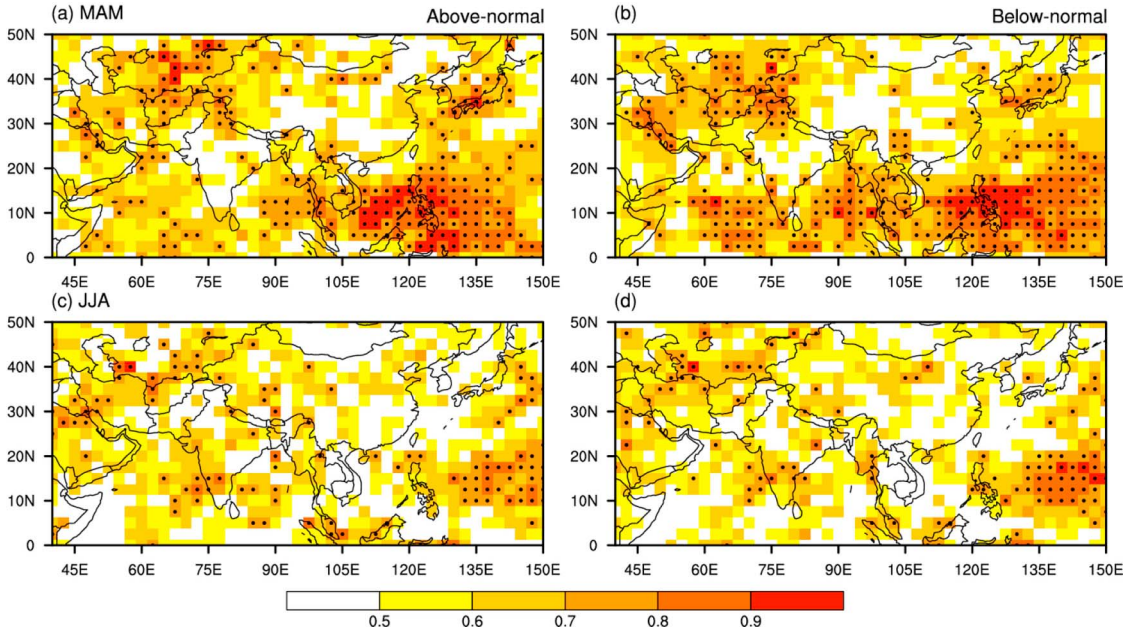

Figure 2. ROCS of the PMMP for (a, b) MAM and (c, d) JJA precipitation for AN (Figures 2a and 2c) and BN categories (Figures 2b and 2d). The black dots indicate grid points for which ROCS is significant at the 95% confidence level, which was obtained by a Monte Carlo test with 500 random trials.

which the forecasts are grouped. The diagonal connecting the points (0, 0) and (1, 1) represents the perfect forecast, i.e., for resolution and reliability. Thus, the closer the curve to the diagonal, the higher is the skill of the forecast. The ROC is the signal detection curve obtained by plotting a graph of hit rate against false alarm rate over a range of different probability thresholds. To assess the skill of the forecasts against climatological forecasts in each category, we use the Brier skill score (BSS) [*Murphy*, 1973; *Stanski et al.*, 1989] (detailed descriptions are given by *Wilks* [1995]). The statistical significance of the obtained verification scores was assessed using the Monte Carlo approach [*Stephenson and Doblas-Reyes*, 2000]. For this, we randomly scrambled the forecast fields 500 times in the time domain.

3. Evaluation of the PMMP

[13] *Wang et al.* [2009] demonstrated that BSS and ROCS—two skill metrics for probabilistic forecasts—yield a similar spatial distribution of skills and are also similar to the pattern associated with the temporal correlation coefficient (TCC), a skill measure of deterministic MME forecasts. Thus, to begin with, we examine the TCC skill of the MME comprising the four coupled models for predicting MAM and JJA precipitation with February initial conditions, for the hindcast period of 1983–2005. Here, the MME average was computed using the simple composite method (i.e., with equal weights for all models).

[14] From the results shown in Figure 1, it can be seen that the deterministic MME has much better skill in MAM than in JJA, especially from the eastern Indian Ocean to the western Pacific Ocean and over Central Asia, some parts of East Asia (including Korea and Japan), and central to eastern north China (adjoining Mongolia). We also compared the TCC skills for the MME prediction based on all years (Figures 1a and 1b; totally 23 years), those after the mature phase of ENSO (Figures 1c and 1d; totally 15 years; see also section 2.3), and also the remaining normal seasons (8 years). The similarity between the results for all years and only those after mature ENSO events suggests that the coupled models' skill mainly comes from their ability in capturing the impact of ENSO. For MAM precipitation, their skill over the western Pacific after the peak of ENSO is even higher than that based on the whole hindcast record. The lagged impact of ENSO on the ASM rainfall in the model environments still remained significant in the subsequent JJA season, although the models had lower skill in most continental Asian locations. In contrast, for normal years, it was found that the one-month lead MAM forecast skill is not better than the four-month lead JJA forecast skill (figures not shown).

[15] Figure 2 shows the general performance of the PMMP in predicting seasonal precipitation in terms of the spatial distribution of the ROCS. Most areas with significant skill in MAM prediction are located in the region from the eastern Indian Ocean to the western Pacific Ocean and over Central Asia and some parts of East Asia for the AN category (Figure 2a). Similarly, the skill for the BN category occupied most of the abovementioned locations as well as the western Indian Ocean. It is noted that the ROCS plots for the AN and BN categories display patterns very similar to the TCC score of the MAM deterministic forecast (see Figure 1a). For JJA, the skill of the probabilistic MME decreases drastically, especially over continental Asia. Overall, the above analysis reveals that the coupled model MME is capable of predicting MAM mean precipitation over some parts of Asia with high fidelity, but has difficulties in predicting JJA mean rainfall over most ASM locations.

[16] Figure 3 shows regionally aggregated reliability diagrams for the PMMP with the corresponding frequency

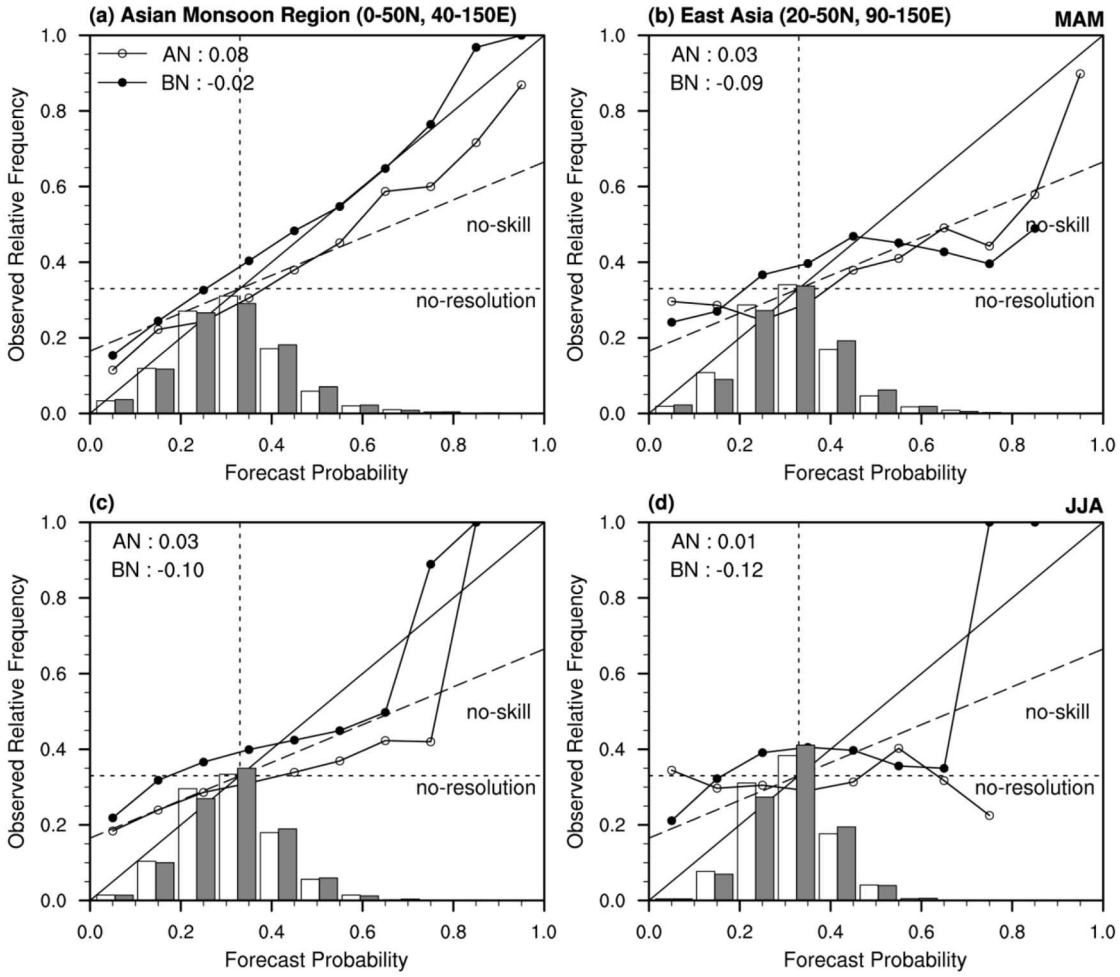

Figure 3. Reliability diagram and frequency histogram for the PMMP for (a, b) MAM and (c, d) JJA precipitation for the ASM region (0°–50°N, 40°–150°E) (Figures 3a and 3c) and East Asia (20°–50°N, 90°–150°E) (Figures 3b and 3d). White (gray) bars and open (closed) circles indicate relative frequency and reliability for the AN (BN) category, respectively. The area-averaged values of BSS over each region are provided to the upper left of each panel.

histograms for the Asia monsoon region (0°–50°N, 40°–150°E) and East Asia (20°–50°N, 90°–150°E). The PMMP generally underestimates (i.e., above the diagonal line) in low probability and overestimates (i.e., below the diagonal line) in high probability compared with the observed relative frequency (except the AN category for MAM over the ASM region). For MAM precipitation, the PMMP curve only deviates slightly from the diagonal. In addition, for the AN and the BN categories, the MAM precipitation forecasts outperform climatology (i.e., reliability is equal to resolution) over the ASM region and are definitely more skillful than random forecasts (i.e., no resolution) over East Asia. The skill of the PMMP for JJA precipitation is lower than that for MAM; however, note that the JJA precipitation forecasts are still more skillful than random guesses over the ASM region for both categories. Curves of both categories for East Asian JJA precipitation are out of phase. The AN curve even falls beneath the no-resolution line for high probability, exhibiting minimal resolution. To quantify the bias of the PMMP, we also evaluated the BSS value for each category. The regionally aggregated BSS values of the PMMP are shown in the top-left corner of the plots. For the AN category, the MAM and JJA precipitation forecasts are more skillful than those for the BN category in both regions (i.e., positive BSS indicates that the PMMP outperforms climatological forecasts in the AN category). In addition, the analyses show that the predictions become less reliable as the forecast lead time increases for both regions.

[17] Regionally aggregated ROC curves and their ROCS were also used to assess performance of the PMMP during the hindcast period (results not shown). The ROC curves were found to be consistent with the reliability diagrams (see Figure 3). For the MAM forecast, the curve is farther away from the diagonal, deviated to the left and upward, compared with its JJA counterpart. The regionally aggregated ROCS for the MAM forecast are much higher than for the JJA forecast and are also above 0.5 (i.e., the value for no-skill forecast), so that the forecast could be considered skillful. In contrast, ROCS for the JJA forecast over the ASM region and East Asia are relatively low with values of 0.55 (0.55) and 0.51 (0.51) for AN (BN), respectively.

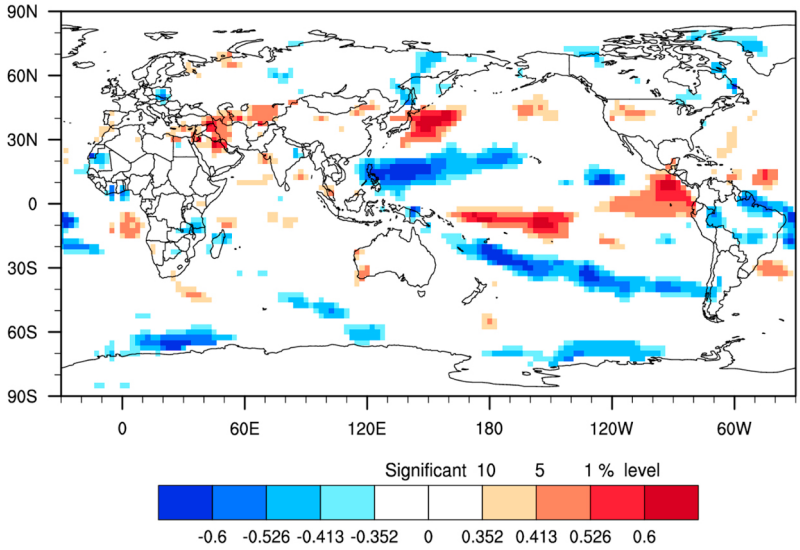

Figure 4. TCC between Nino 3.4 index for the preceding DJF and the mean precipitation in the following JJA season. Values with absolute magnitudes of 0.526, 0.413, and 0.352 represent the 99%, 95%, and 90% confidence levels, respectively.

[18] In summary, we examined the forecast skills of the deterministic MME prediction and the PMMP for the ASM precipitation. Our results reveal that coupled models are capable of predicting the ASM rainfall variability during MAM but not JJA. It is noticed that the forecast skill mainly stems from the coupled models' ability to capture climate anomalies after the mature phase of ENSO. However, the forecasts exhibit very low skill after normal winters in both MAM and JJA.

4. Evaluation of the Statistical Model

[19] To develop a statistical model for predicting the ASM precipitation, we first investigated the lagged impact of ENSO on the precipitation. Figure 4 shows the temporal correlation coefficient between the DJF Niño 3.4 index and precipitation in the following JJA. Positive correlation is found over Western to Central Asia, Northeast Asia adjoining the WNP, and the equatorial central and eastern Pacific regions adjacent to Latin America. Negative signals are found in the tropical western Pacific, in the South Pacific trailing the South Pacific convergence zone (SPCZ), and over parts of Brazil. It is noteworthy that strong signals are found over the western Pacific, consistent with previous studies showing that the East Asian summer monsoon variations are linked to decaying El Niño or La Niña [*Wang*

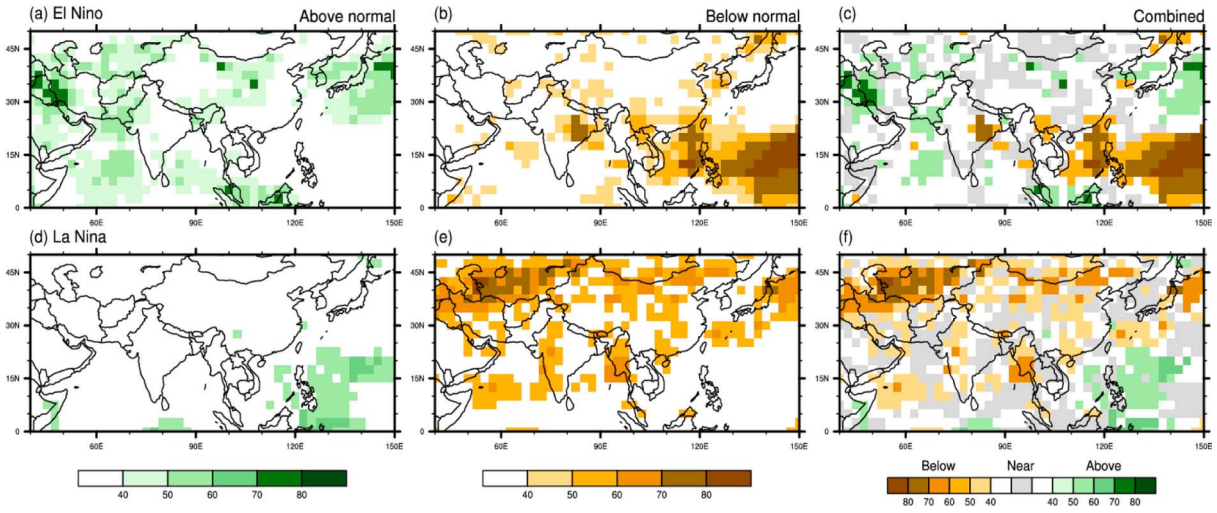

Figure 5. Conditional probabilistic composites of the JJA seasonal mean precipitation after mature phase of ENSO for (top) El Niño and (bottom) La Niña years for (a, d) AN and (b, e) BN categories. (c, f) Combined maps showing regions where either the AN, NN, or BN category is dominant, based on Pearson's chi-square (χ^2) test.

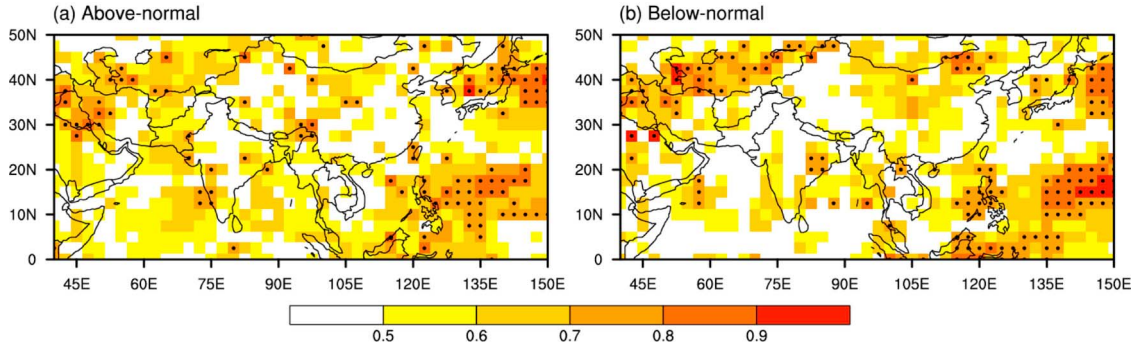

Figure 6. ROCS of the statistical model for the JJA mean precipitation for (a) AN and (b) BN categories.

et al., 2004, 2008, 2009; *J.-Y. Lee et al.*, 2011; *S. S. Lee et al.*, 2011; *Lee and Wang*, 2012; *Chowdary et al.*, 2010].

[20] To depict the precipitation patterns related to the ENSO condition in the previous winter, probabilistic composites were computed by ranking JJA mean precipitation in selected years for which the preceding DJF Niño 3.4 index was −0.5 (+0.5) standard deviations below (above) average (see also section 2). Figure 5 shows the probabilistic composites of JJA mean precipitation over the ASM region for the AN and BN categories after the mature phase of ENSO during the training period. The regional distribution of probabilistic composites associated with El Niño for the AN category mainly shows wetter-than-normal conditions over the Indian Ocean, Central Asia, central China, and the WNP region covering Korea and the Japanese archipelago. The strongest signals for the BN category are found more eastward that for AN, and show drier-than-normal conditions along coastal East Asia (spanning Korea, Taiwan, and southern China), as well as over eastern India and the tropical western Pacific. However, the impact of La Niña manifested as drier-than-normal conditions over many parts of the ASM region. No significant signal appeared for the AN category except over the Philippines and the adjoining the tropical western Pacific.

[21] In summary, the lagged impact of El Niño on the ASM precipitation is characterized by a more local response that includes above normal probabilities over the western Indian Ocean, Central Asia, western-to-central part of northern China, and Northeast Asia, and below normal probabilities from the western tropical Pacific extending into Indochina. However, it is more likely for continental Asia to experience drier-than-normal conditions after the mature phase of La Niña.

[22] The statistical model was developed by projecting the status of the preceding ENSO onto a composite map produced by leave-one-year-out cross-validation, as described in section 2.2. It is interesting to note that the statistical model has better skill than the dynamical models, especially over Northeast Asia and some part of Southeast Asia during the cross-validation period, as shown in Figure 6. This is consistent with the statistical model performance in seasonal forecasting of southwest monsoon rainfall over India [*Rajeevan et al.*, 2007]. Because of the design of the statistical model, the spatial distribution of its forecast skill for the two categories is similar to that of the observed probability composites for El Niño and La Niña (Figure 5). Further assessment of the statistical model prediction for MAM precipitation revealed much higher skill for the forecast

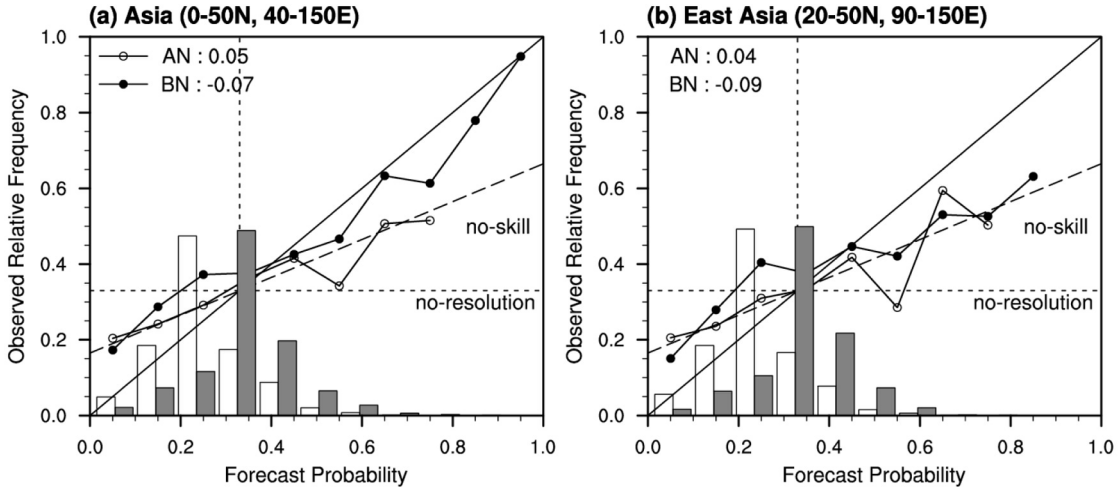

Figure 7. Reliability diagram and frequency histogram for the statistical model for JJA mean precipitation over (a) the ASM region and (b) East Asia.

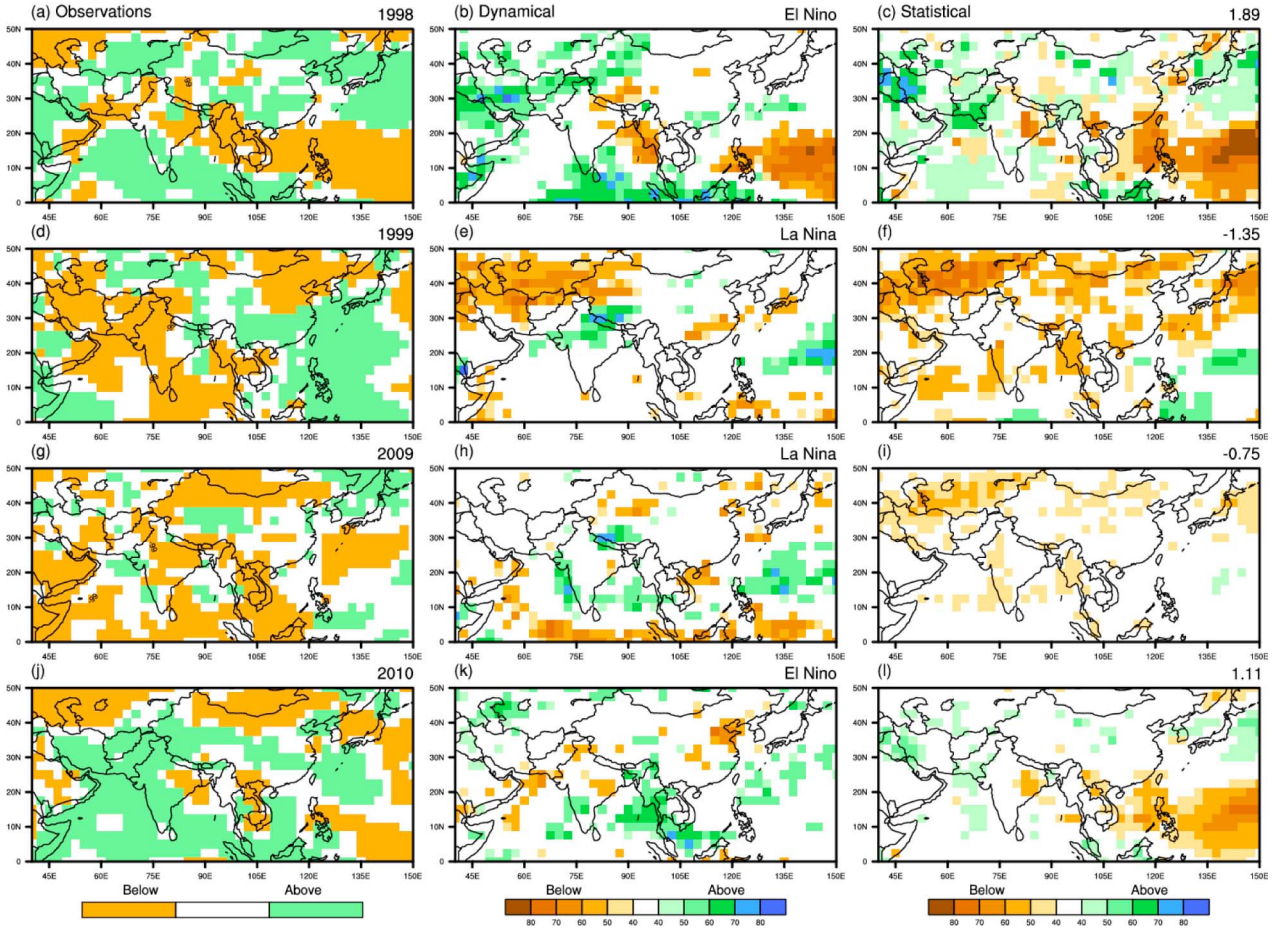

Figure 8. Anomalous JJA mean precipitation from (a, d, g, j) observations, and probabilities (%) from (b, e, h, k) PMMP, and (c, f, i, l) the statistical model for the years 1998 and 1999 (hindcast), and for 2009 and 2010 (real-time forecast). Probabilities for both AN and BN categories are shown in the same map for the PMMP and the statistical model predictions. Standardized Niño 3.4 indices for the preceding DJF seasons are provided to the upper right of the right panels.

based on the recent physical relation than those with a long lag, despite using the same predictor (figures not shown). This suggests that the physical relation may weaken due to accumulation of uncertainties as the lag time increases.

[23] The performance of the statistical model for boreal summer precipitation was also assessed using regionally aggregated reliability diagrams and ROC curves for the cross-validation period. In comparison with the PMMP, there are three interesting features. First, the statistical prediction also underestimates in low probability and overestimates in high probability, similar to the PMMP (Figure 7). Second, the statistical model has better reliability and resolution than the PMMP for both AN and BN categories. In terms of ROCS, the statistical model is better than the PMMP, especially over East Asia, where the PMMP has marginal skill close to 0.5 (figure not shown). Third, the statistical model performs better for AN than BN events in Asian and East Asian locations, whereas the PMMP has similar skill for both categories.

[24] The results here show that, in general, the statistical model outperforms the PMMP during the hindcast period of 1983–2005. However, its skill may be overestimated due to overfitting, even though cross-validation was used to assess the statistical model.

5. Comparison of Dynamical and Statistical Prediction

[25] Next we compared the PMMP and the statistical model during the hindcast as well as the real-time forecast period. However, since the real-time coupled MME product has been available for only a few years, there are insufficient samples for a quantitative estimate and a well-grounded conclusion. Nonetheless, it is still worthwhile to examine the recent real-time operational forecasts. We first show case studies for two summers after the mature phase of El Niño (1998 and 2010) and two summers after the mature phase of La Niña (1999 and 2009) (see Figure 8).

[26] The two summers after the mature phase of El Niño selected here exhibit quite different precipitation anomalies in the observations, particularly over East Asia. The summer of 1998 exhibited the typical pattern of the decaying El Niño impact, with wetter-than-normal conditions over East Asia, some parts of the Indian subcontinent, and the Indian Ocean,

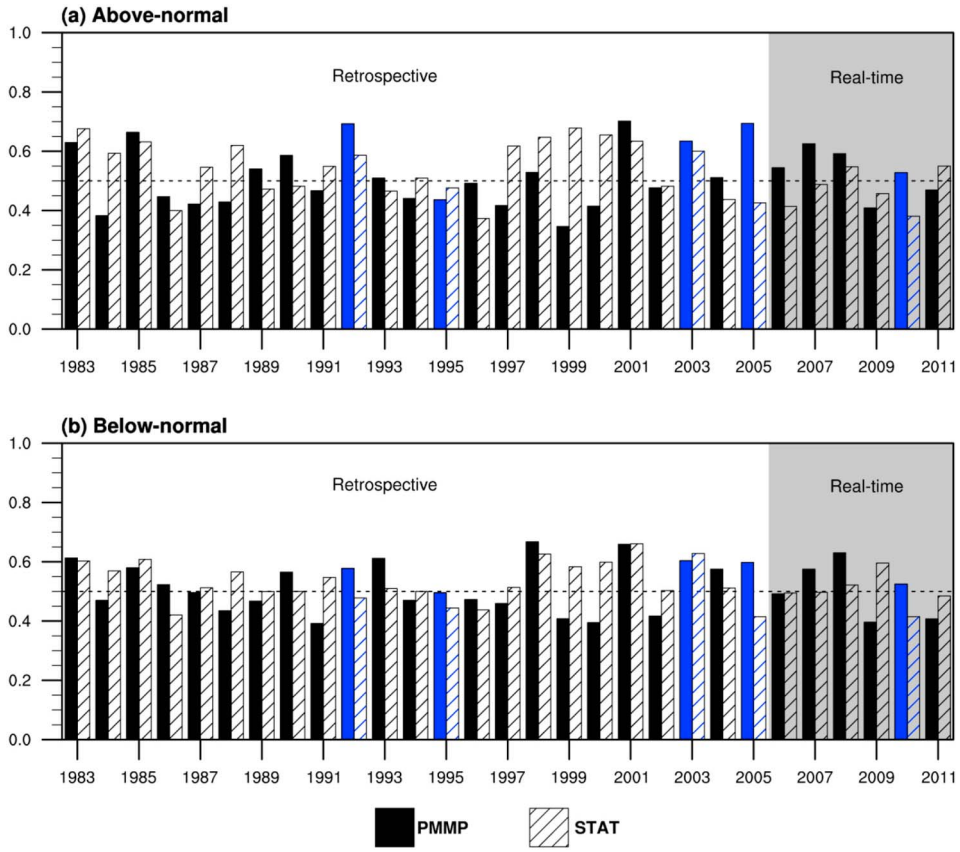

Figure 9. ROCS of historical (1983–2005) and real-time (2006–2011) JJA mean precipitation predictions for (a) AN and (b) BN categories for East Asia (20°–50°N, 90°–150°E). Solid bars denote the PMMP and hatched bars denote the statistical model forecasts. Blue bars indicate the summers after the peak of El Niño Modoki events. Dashed line corresponds to climatological forecast.

together with drier-than-normal conditions over the Bay of Bengal, South China Sea, Philippines Sea, and tropical Western Pacific. Further, although the summer of 1998 had a dipole pattern of anomalous precipitation over the tropical western Pacific and East Asia, the summer of 2010 had a triple pattern over the same region. It has been suggested that the 2009/10 event might have been an atypical El Niño, i.e., El Niño Modoki [*Ashok et al.*, 2007] or Central-Pacific-type El Niño [*Yu and Kao*, 2007; *Kao and Yu*, 2009], which yields different patterns of sea-surface warming and cooling in the tropical Pacific and has impacts on different extratropical regions. Further, it is interesting to note that the PMMP has better skill than the statistical model for the summer of 2010, whereas the statistical model is more skillful for the summer of 1998. This suggests that the statistical model is unable to capture the impact of an atypical ENSO on precipitation over the WP-EA region.

[27] The results for the two summers after the mature phase of La Niña (1999 and 2009) indicate that the current statistical model is more useful for predicting below-normal precipitation conditions over many parts of Asia. In the summer of 1999, below-normal conditions were found over continental Asia (except southern China) and above-than-normal conditions were seen over the Philippines and the surrounding areas. In the statistical prediction, La Niña shows great impact on the drier-than-normal conditions over continental Asia, and the dry signals over parts of western Asia, Mongolia, and northeast China are consistent with observations. The PMMP, however, predicts below-normal rainfall only over parts of western Asia, but near normal or uncertain rainfall over most of continental Asia. The observed pattern for the summer of 2009 is similar to that in 1999, indicating below-normal conditions over most of continental Asia (except western China). Since the magnitudes of the Niño 3.4 indices for 1998/99 and 2008/09 are different, the strength of the impacts associated with La Niña events given by the statistical models are also different. In other words, the patterns of the statistical model are consistent, but the strengths of the associated patterns are different. In contrast, the PMMP indicates that most of the ASM region has near normal or uncertain rainfall.

[28] Figure 9 summarizes the skill comparison between the PMMP and the statistical model for both the hindcast (or cross-validated) period (1983–2005) and the real-time (or independent) period (2006–2011). First, it can be seen that the statistical model has generally better skill for JJA precipitation over the East Asian region in both AN and BN categories during the hindcast period. However, the PMMP is more skillful after the mature phase of an atypical ENSO such as in the summers of 1992, 2003, and 2005. Second, the PMMP also seems to have better skill during the independent forecast period of 2006–2011, partly suggesting that

Table 2. ROCS of the PMMP and Statistical JJA Mean Precipitation Forecasts for the AN and BN Categories for the Period Covering Both Historical and Real-Time Forecasts[a]

	AN		BN	
	PMMP	Statistical	PMMP	Statistical
		ASM Region		
All years	0.55 (0.54)	0.55 (0.55)	0.54 (0.54)	0.56 (0.56)
El Niño years	0.55 (0.57)	0.60 (0.60)	0.56 (0.57)	0.59 (0.60)
Neutral years	0.56 (0.55)	0.50 (0.50)	0.55 (0.54)	0.50 (0.50)
La Niña years	0.53 (0.52)	0.56 (0.57)	0.52 (0.51)	0.57 (0.58)
		East Asia Region		
All years	0.52 (0.52)	0.53 (0.55)	0.52 (0.52)	0.53 (0.53)
El Niño years	0.54 (0.54)	0.57 (0.59)	0.55 (0.56)	0.53 (0.55)
Neutral years	0.53 (0.51)	0.50 (0.50)	0.52 (0.51)	0.50 (0.50)
La Niña years	0.50 (0.50)	0.53 (0.55)	0.49 (0.50)	0.54 (0.55)

[a]Values in parentheses are the ROCS for historical forecasts only.

cross-validation may overestimate the forecast skill of the statistical model. The relatively lower skill with the statistical model for this period may also be due to the shift in the conventional ENSO pattern, which may not be well presented.

[29] The dependency of the forecast skills on the ENSO phase was further investigated. Table 2 gives a summary of the PMMP and statistical model forecast skills during summers after the mature phase of El Niño and La Niña and after normal winters. First, the statistical forecast is more sensitive to the ENSO phase. The statistical model has the highest skill during summers after the mature phase of El Niño but the lowest skill during summers after normal winters over both the ASM region and East Asia. Second, the PMMP exhibits the lowest skill during summers after the mature phase of La Niña over the ASM and East Asian regions. During neutral years, the PMMP has better skill than the statistical model, whereas the statistical model performs better during summers after El Niño or La Niña. These results suggest that the statistical model has considerable potential for improving long-lead predictions of the ASM precipitation. However, it is also clear that the PMMP performs better in summers after normal or atypical ENSO winters.

6. Summary and Discussion

[30] The long-lead probabilistic predictions of the APCC multimodel system and the statistical model for the ASM precipitation during 1983–2011 were assessed. Particular attention was paid to the probabilistic prediction of precipitation in summer after the mature phase of ENSO. It is found that the general patterns of prediction skill of the coupled models for MAM and JJA precipitation in all years are almost the same as those computed for seasons after mature phase of ENSO. However, the skill for MAM is not higher than that for JJA after ENSO-neutral winters. This suggests that the skill of the coupled models in predicting MAM and JJA precipitation mainly comes from their ability of capturing ENSO teleconnection.

[31] Previous studies have suggested that the ASM precipitation in summers after the mature phase of ENSO tends to be more predictable. We therefore developed the simple lag-regression-based empirical probabilistic forecast model for the ASM precipitation using the preceding winter ENSO condition as the predictor. We found that the regional distributions of the probabilistic composites associated with El Niño and La Niña were not mirror images of each other. After the peak phase of El Niño, the composite patterns indicated wetter-than-normal conditions over the Indian Ocean, Central Asia, central part of northern China, Northeast Asia, Korea, and Japan, but below-normal rainfall along coastal East Asia, eastern India, and the tropical western Pacific. A basic understanding of the simultaneous influence of El Niño on the ASM suggests that the monsoon rainfall should be substantially deficient, yet this was not often the case for the Indian monsoon because of other local factors [*Slingo and Annamalai*, 2000]. After the peak of La Niña, drier-than-normal conditions are more likely in many locations in continental Asia.

[32] The comparison between the PMMP and statistical model in terms of the ASM precipitation forecast indicates that, in general, the statistical model outperforms the PMMP for the retrospective forecast period, whereas the PMMP is more skillful during the real-time forecast period of the last 6 years, for both the AN and BN categories. This may indicate that the cross-validated statistical prediction cannot avoid overfitting. The relatively lower skill of the statistical model for the later period may also be due to the shift in the conventional ENSO pattern, which is not well presented by the model. The statistical forecast is more sensitive to the ENSO phase and proves useful with regard to La Niña-related teleconnection. However, it cannot properly capture the atmospheric impact due to atypical ENSO during the early 1990s and in the recent decade. In contrast, the PMMP exhibits the lowest skill during summers after the mature phase of La Niña, but gives a more stable and consistent forecast skill even during atypical ENSO or normal years.

[33] Since the statistical model depends on the selection of potential predictors and the available training period [*Rajeevan et al.*, 2007], it should be designed and assessed carefully to avoid artificial predictability. In view of the preconditions, *Kung and Sharif* [1982] and *McBride and Nicholls* [1983] highlighted the need for regular training or updating of the forecast models with the latest data for better forecasts. Furthermore, *Nicholls* [1984] and *Rajeevan et al.* [2007] identified the near optimal length for the training period according to their own experimental designs. In particular, the necessity for updating model equations stems from the fact that the time series of meteorological parameters are statistically nonstationary.

[34] Because the statistical model adopted here uses the ENSO phase in the preceding boreal winter as the predictor and was trained for the historical 23 years (covering the same period of 1983–2005 to provide a corresponding prediction to the hindcast of the PMMP), it might not be able to capture signals associated with other climate modes or impacts due to the changing background climate. For instance, the East Asian summer monsoon can also be affected by simultaneous local SST variability [*S. S. Lee et al.*, 2011], North Atlantic Oscillation (NAO; *Wu et al.* [2009]), and Eurasian pattern activity [*Lee et al.*, 2005; *Min and Jhun*, 2010]. Regional and planetary scale features of the atmosphere–ocean system for the monsoon season, such as the prevailing circulation over the midlatitudes of Eurasia and the South Indian Ocean as well as anomalous

warmer SST over the WNP region and ENSO, could contribute to the monsoon drought over India [*Sikka*, 2003]. There has also been a decadal change in the East Asia-WNP summer monsoon relationship from an ENSO-related oscillation in 1979–1993 to a monsoon-dominated oscillation in 1994–2004 [*Kwon et al.*, 2005]. Also, the inverse relationship between ENSO and the Indian summer monsoon has broken down in recent decades [*Kumar et al.*, 1999]. Moreover, some of the recent Pacific warming events have shown different characteristics compared to the conventional El Niño [*Ashok and Yamagata*, 2009], which leads to different impacts on the East Asian rainfall after the peak of ENSO [*Feng et al.*, 2011].

[35] Finally, it is worthwhile to assess the skill of the PMMP, which comprises state-of-the-art coupled models, and to compare it with the pure statistical model, focusing on the ASM precipitation after the mature phase of ENSO. The statistical model, which trades off goodness-of-fit against stability, has potential for improving long-lead predictions. However, the PMMP is more stable, and, in particular, the dynamical ENSO prediction skills are reasonably good on long-range time scales of 6 months or beyond. Therefore, to improve the long-lead ASM precipitation forecast skills, statistical post-processing of model outputs (e.g., downscaling) could also be applied by utilizing such relatively predictable information from a dynamical model as the predictor.

[36] **Acknowledgments.** The authors appreciate those institutes, including NCEP, FRCGC, and SNU, participating in the APCC coupled 6-month multimodel ensemble prediction system for providing the hindcast/forecast experimental data. Lee and Wang acknowledge support from IPRC, which is in part supported by JAMSTEC, NOAA (grant NNX07AG53G), and NASA (grant NA09OAR4320075). Tam acknowledges the support from the City University of Hong Kong (grant 9360126). This is the IPRC publication 834 and the SOEST publication 8534.

References

Alessandri, A., A. Borrelli, A. Navarra, A. Arribas, M. Déqué, P. Rogel, and A. Weisheimer (2011), Evaluation of probabilistic quality and value of the ENSEMBELS multimodel seasonal forecasts: Comparison with DEMETER, *Mon. Weather Rev.*, *139*, 581–607, doi:10.1175/2010MWR3417.1.

Anderson, J., H. van den Dool, A. G. Barnston, W. Chen, W. Stern, and J. Ploshay (1999), Present-day capabilities of numerical and statistical models for atmospheric extratropical seasonal simulation and prediction, *Bull. Am. Meteorol. Soc.*, *80*(7), 1349–1361, doi:10.1175/1520-0477(1999)080<1349:PDCONA>2.0.CO;2.

Ashok, K., and T. Yamagata (2009), The El Nino with a difference, *Nature*, *461*, 481–484, doi:10.1038/461481a.

Ashok, K., S. K. Behera, S. A. Rao, H. Weng, and T. Yamagata (2007), El Niño Modoki and its possible teleconnection, *J. Geophys. Res.*, *112*, C11007, doi:10.1029/2006JC003798.

Atger, F. (2003), Spatial and interannual variability of the reliability of ensemble-based probabilistic forecasts: Consequences for calibration, *Mon. Weather Rev.*, *131*, 1509–1523, doi:10.1175//1520-0493(2003)131<1509:SAIVOT>2.0.CO;2.

Atger, F. (2004), Estimation of the reliability of ensemble based probabilistic forecasts, *Q. J. R. Meteorol. Soc.*, *130*, 627–646, doi:10.1256/qj.03.23.

Barnston, A. G., M. H. Glantz, and Y. He (1999), Predictive skill of statistical and dynamical climate models in SST forecasts during the 1997–98 El Nino episode and the 1998 La Nino onset, *Bull. Am. Meteorol. Soc.*, *80*, 217–243, doi:10.1175/1520-0477(1999)080<0217:PSOSAD>2.0.CO;2.

Chowdary, J., S. P. Xie, J. Y. Lee, Y. Kosak, and B. Wang (2010), Predictability of summer Northwest Pacific climate in eleven coupled model hindcasts: Local and remote forcing, *J. Geophys. Res.*, *115*, D22121, doi:10.1029/2010JD014595.

Climate Test Bed (2006), Multi-model ensembles: Transition from research to operations and implementation strategy, report, NOAA, Silver Spring, Md. [Available at http://www.cpc.noaa.gov/products/ctb/ctb-publications.shtml.]

Doblas-Reyes, F. J., M. Deque, and J. P. Piedelievre (2000), Multi-model spread and probabilistic seasonal forecasts in PROVOST, *Q. J. R. Meteorol. Soc.*, *126*, 2069–2088, doi:10.1256/smsqj.56704.

Feng, J., W. Chen, C. Y. Tam, and W. Zhou (2011), Different impacts of El Niño and El Niño Modoki on China rainfall in the decaying phases, *Int. J. Climatol.*, *31*, 2091–2101, doi:10.1002/joc.2217.

Graham, R. J., et al. (2005), A performance comparison of coupled and uncoupled versions of the Met Office seasonal prediction general circulation model, *Tellus, Ser. A*, *57*(3), 320–339, doi:10.1111/j.1600-0870.2005.00116.x.

Green, D. M., and J. A. Swets (1966), *Signal Detection Theory and Psychophysics*, Wiley, New York.

Ham, Y. G., and I. S. Kang (2010), Improvement of seasonal forecasts with inclusion of tropical instability waves on initial conditions, *Clim. Dyn.*, *36*(7–8), 1277–1290, doi:10.1007/s00382-010-0743-0.

Janowiak, J. E., and P. Xie (1999), CAMS_OPI: A global satellite-rain gauge merged product for real-time precipitation monitoring applications, *J. Clim.*, *12*, 3335–3342, doi:10.1175/1520-0442(1999)012<3335:COAGSR>2.0.CO;2.

Jeong, H. I., et al. (2008), Experimental 6-month hindcast and forecast simulation using CCSM3, *APCC 2008 Tech. Rep*, APEC Clim. Cent., Pusan, South Korea.

Jin, E. K., et al. (2008), Current status of ENSO prediction skill in coupled ocean-atmosphere models, *Clim. Dyn.*, *31*(6), 647–664, doi:10.1007/s00382-008-0397-3.

Jolliffe, I. T., and D. B. Stephenson (2003), *Forecast Verification*, John Wiley, Chichester, U. K.

Kao, H. Y., and J. Y. Yu (2009), Contrasting eastern-Pacific and central-Pacific types of ENSO, *J. Clim.*, *22*, 615–632, doi:10.1175/2008JCLI2309.1.

Krishnamurti, T. N., et al. (1999), Improved weather and seasonal climate forecasts from multi-model superensemble, *Science*, *285*, 1548–1550, doi:10.1126/science.285.5433.1548.

Krishnamurti, T. N., C. M. Kishtawal, D. W. Shin, and C. E. Williford (2000), Multi-model superensemble forecasts for weather and seasonal climate, *J. Clim.*, *13*, 4196–4216, doi:10.1175/1520-0442(2000)013<4196:MEFFWA>2.0.CO;2.

Krzysztofowicz, R. (1983), Why should a forecaster and a decision maker use Bayes theorem, *Water Resour. Res.*, *19*, 327–336, doi:10.1029/WR019i002p00327.

Kug, J. S., J. Y. Lee, I. S. Kang, B. Wang, and C. K. Park (2008), Optimal multi-model ensemble method in seasonal climate prediction, *Asia-Pac. J. Atmospheric Sci.*, *44*, 259–267.

Kumar, K. K., B. Rajagopalan, and M. A. Cane (1999), On the weakening relationship between the Indian monsoon and ENSO, *Science*, *284*, 2156–2159, doi:10.1126/science.284.5423.2156.

Kung, E. C., and T. A. Sharif (1982), Long range forecasting of the Indian summer monsoon onset and rainfall with upper air parameters and SST, *J. Meteorol. Soc. Jpn.*, *60*, 672–681.

Kwon, M. H., J. G. Jhun, B. Wang, S. I. An, and J. S. Kug (2005), Decadal change in relationship between east Asian and WNP summer monsoon, *Geophys. Res. Lett.*, *32*, L16709, doi:10.1029/2005GL023026.

Lee, E. J., J. G. Jhun, and C. K. Park (2005), Remote connection of the northeast Asian summer rainfall variation reveled by a newly defined monsoon index, *J. Clim.*, *18*, 4381–4393, doi:10.1175/JCLI3545.1.

Lee, J.-Y., and B. Wang (2012), Seasonal climate prediction and predictability of atmospheric circulation, in *Climate Models*, edited by L. M. Druyan, InTech, Rijeka, Croatia, in press.

Lee, J.-Y., et al. (2010), How are seasonal prediction skills related to models' performance on mean state and annual cycle?, *Clim. Dyn.*, *35*, 267–283, doi:10.1007/s00382-010-0857-4.

Lee, J.-Y., B. Wang, Q. Ding, K. J. Ha, J. B. Ahn, A. Kumar, B. Stern, and O. Alves (2011), How predictable is the Northern Hemisphere summer upper-tropospheric circulation?, *Clim. Dyn.*, *37*, 1189–1203, doi:10.1007/s00382-010-0909-9.

Lee, S. S., J. Y. Lee, K. J. Ha, B. Wang, and J. K. E. Schemm (2011), Deficiencies and possibilities for long-lead coupled climate prediction of the Western North Pacific-East Asian summer monsoon, *Clim. Dyn.*, *36*, 1173–1188, doi:10.1007/s00382-010-0832-0.

Lee, W. J., et al. (2009), APEC 2009 final report, report, APEC Clim. Cent., Pusan, South Korea. [Available at http://www.apcc21.net/en/activities/publications/reports/].

Liang, J., S. Yang, Z. Z. Hu, B. Huang, A. Kumar, and Z. Zhang (2009), Predictable patterns of the Asian and Indo-Pacific summer precipitation in the NCEP CFS, *Clim. Dyn.*, *32*, 989–1001, doi:10.1007/s00382-008-0420-8.

Luo, J. J., et al. (2005), Seasonal climate predictability in a coupled OAGCM using a different approach for ensemble forecasts, *J. Clim.*, *18*, 4474–4497, doi:10.1175/JCLI3526.1.

Mason, I. (1982), A model for assessment of weather forecast, *Aust. Meteorol. Mag.*, *30*, 291–303.

Mason, S. J., and N. E. Graham (1999), Conditional probabilities, relative operating characteristics, and relative operating level, *Weather Forecast.*, *14*, 713–725, doi:10.1175/1520-0434(1999)014<0713:CPROCA>2.0.CO;2.

McBride, J. L., and N. Nicholls (1983), Seasonal relationships between Australian rainfall and the Southern oscillation, *Mon. Weather Rev.*, *111*, 1998–2004, doi:10.1175/1520-0493(1983)111<1998:SRBARA>2.0.CO;2.

Min, H. J., and J. G. Jhun (2010), The change in the East Asian summer monsoon simulated by the MIROC3.2 high-resolution coupled model under global warming scenarios, *Asia-Pac. J. Atmos. Sci.*, *46*, 73–88, doi:10.1007/s13143-010-0008-1.

Min, Y. M., V. N. Kryjov, and C. K. Park (2009), A probabilistic multimodel ensemble approach to seasonal prediction, *Weather Forecast.*, *24*, 812–828, doi:10.1175/2008WAF2222140.1.

Murphy, A. H. (1973), A new vector partition of the probability score, *J. Appl. Meteorol.*, *12*, 595–600, doi:10.1175/1520-0450(1973)012<0595:ANVPOT>2.0.CO;2.

Murphy, A. H. (1977), The value of climatological, categorical, and probabilistic forecasts in the cost-loss ration situation, *Mon. Weather Rev.*, *105*, 803–816, doi:10.1175/1520-0493(1977)105<0803:TVOCCA>2.0.CO;2.

Murphy, A. H., and R. L. Winkler (1977), Reliability of subjective probability forecasts of precipitation and temperatures, *Appl. Stat.*, *26*, 41–47, doi:10.2307/2346866.

Nicholls, N. (1984), The stability of empirical long range forecast techniques: A case study, *J. Appl. Meteorol.*, *23*, 143–147, doi:10.1175/1520-0450(1984)023<0143:TSOELR>2.0.CO;2.

Palmer, T. N., C. Brankovic, and D. S. Richardson (2000), A probability and decision-model analysis of PROBOST seasonal multi-model ensemble integrations, *Q. J. R. Meteorol. Soc.*, *126*, 2013–2033, doi:10.1256/smsqj.56702.

Palmer, T. N., et al. (2004), Development of a European multi-model ensemble system for seasonal to inter-annual prediction, *Bull. Am. Meteorol. Soc.*, *85*, 853–872, doi:10.1175/BAMS-85-6-853.

Rajeevan, M., D. S. Pai, R. Anil Kumar, and B. Lal (2007), New statistical models for long-range forecasting of southwest monsoon rainfall over India, *Clim. Dyn.*, *28*, 813–828, doi:10.1007/s00382-006-0197-6.

Reynolds, R. W., N. A. Rayner, T. M. Smith, D. C. Stokes, and W. Wang (2002), An improved in situ and satellite SST analysis for climate, *J. Clim.*, *15*, 1609–1625, doi:10.1175/1520-0442(2002)015<1609:AIISAS>2.0.CO;2.

Richardson, D. S. (2000), Skill and economic value of the ECMWF ensemble prediction system, *Q. J. R. Meteorol. Soc.*, *126*, 649–667, doi:10.1002/qj.49712656313.

Richardson, D. S. (2006), Predictability and economic value, in *Predictability of Weather and Climate*, edited by T. Palmer and R. Hagedorn, pp. 628–644, Cambridge Univ. Press, Cambridge, U. K., doi:10.1017/CBO9780511617652.026.

Saha, S., et al. (2006), The NCEP Climate Forecast System, *J. Clim.*, *19*, 3483–3517, doi:10.1175/JCLI3812.1.

Shukla, J., et al. (2000), Dynamical seasonal prediction, *Bull. Am. Meteorol. Soc.*, *81*, 2593–2606, doi:10.1175/1520-0477(2000)081<2593:DSP>2.3.CO;2.

Sikka, D. R. (2003), Evaluation of monitoring and forecasting of summer monsoon over India and a review of monsoon drought of 2002, *Proc. Indian Natl. Sci. Acad., Part A*, *69*, 474–504.

Slingo, J. M., and H. Annamalai (2000), 1997: The El Niño of the century and the response of the Indian summer monsoon, *Mon. Wea. Rev.*, *128*, 1778–1797, doi:10.1175/1520-0493(2000)128<1778:TENOOT>2.0.CO;2.

Sohn, S. J., C. Y. Tam, K. Ashok, and J. B. Ahn (2012), Quantifying the reliability of precipitation datasets for monitoring large-scale East Asian precipitation variations, *Int. J. Climatol.*, doi:10.1002/joc.2380, in press.

Stanski, H., L. Wilson, and W. Burrows (1989), Survey of common verification methods in meteorology, *Tech. Rep. WMO/TD 358*, World Meteorol. Org., Geneva, Switzerland.

Stephenson, D. B., and F. J. Doblas-Reyes (2000), Statistical methods for interpreting Monte Carlo ensemble forecasts, *Tellus, Ser. A*, *52*, 300–322.

Swets, J. A. (1973), The relative operating characteristics in psychology, *Science*, *182*, 990–1000, doi:10.1126/science.182.4116.990.

van Oldenborgh, G. J., M. A. Balmaseda, L. Ferranti, T. N. Stockdale, and D. L. T. Anderson (2005), Did the ECMWF seasonal forecast model outperform statistical ENSO forecast models over the last 15 years?, *J. Clim.*, *18*, 3240–3249, doi:10.1175/JCLI3420.1.

Wang, B., I. S. Kang, and J. Y. Lee (2004), Ensemble simulations of Asian-Australian monsoon variability by 11 AGCMs, *J. Clim.*, *17*, 803–818, doi:10.1175/1520-0442(2004)017<0803:ESOAMV>2.0.CO;2.

Wang, B., J. Y. Lee, I. S. Kang, J. Shukla, N. H. Saji, and C. K. Park (2007), Coupled predictability of seasonal tropical precipitation, *CLIVAR Exch.*, *12*, 17–18.

Wang, B., et al. (2008), How accurately do coupled climate models predict the Asian-Australian monsoon interannual variability?, *Clim. Dyn.*, *30*, 605–619, doi:10.1007/s00382-007-0310-5.

Wang, B., et al. (2009), Advance and prospectus of seasonal prediction: Assessment of the APCC/CliPAS 14-model ensemble retrospective seasonal prediction (1980–2004), *Clim. Dyn.*, *33*, 93–117, doi:10.1007/s00382-008-0460-0.

Wilks, D. S. (1995), *Statistical Methods in the Atmospheric Sciences: An Introduction*, Academic, San Diego, Calif.

World Meteorological Organization (2002), Standardised Verification System (SVS) for Long-Range Forecasts (LRF): New attachment II-9 to the manual on the GDPS, Vol. 1., *WMO 485*, 24 pp., Geneva, Switzerland.

Wu, Z., B. Wang, J. Li, and F. F. Jin (2009), An empirical seasonal prediction model of the east Asian summer monsoon using ENSO and NAO, *J. Geophys. Res.*, *114*, D18120, doi:10.1029/2009JD011733.

Yu, J. Y., and H. K. Kao (2007), Decadal changes of ENSO persistence barrier in SST and ocean heat content indices: 1958–2001, *J. Geophys. Res.*, *112*, D13106, doi:10.1029/2006JD007654.

Zhu, Y., Z. Toth, R. Wobus, D. Richardson, and K. Mylne (2002), The economic value of ensemble-based weather forecasts, *Bull. Am. Meteorol. Soc.*, *83*, 73–83, doi:10.1175/1520-0477(2002)083<0073:TEVOEB>2.3.CO;2.

J.-B. Ahn, Department of Atmospheric Sciences, Pusan National University, 30 Changjeon-dong, Keumjeoung-ku, Busan 609-735, South Korea.

I.-S. Kang, Climate Environment System Research Center, Seoul National University, Seoul 151-742, South Korea.

J.-Y. Lee and B. Wang, International Pacific Research Center, University of Hawai'i at Mānoa, 1680 East-West Rd., POST Bldg. 401, Honolulu, HI 96822, USA. (jylee@soest.hawaii.edu)

Y.-M. Min and S.-J. Sohn, APEC Climate Center, 1463 U-dong, Haeundae-gu, Busan 612-020, South Korea.

C.-Y. Tam, Guy Carpenter Asia-Pacific Climate Impact Centre, City University of Hong Kong, Hong Kong.

T. Yamagata, Department of Earth and Planetary Science, University of Tokyo, 7-3-1 Hongo, Bunkyo-ku, Tokyo 113-0033, Japan.